Solid State Science and Technology, Vol. 17, No 2 (2009) 133-143
ISSN 0128-7389

EPOXIDISED NATURAL RUBBER - ALUMINA NANOPARTICLE COMPOSITES (ENRAN): EFFECT OF FILLER LOADING ON THE TENSILE PROPERTIES

N. Mohamad[1,3], A. Muchtar[1], M.J. Ghazali[1], H.M. Dahlan[2] and C.H. Azhari[1]

[1] *Faculty of Engineering, Universiti Kebangsaaan Malaysia, 43600 Bangi, Selangor, Malaysia*

[2] *Malaysian Nuclear Agency, 43000 Bangi, Selangor, Malaysia*

[3]*Faculty of Manufacturing Engineering, Universiti Teknikal Malaysia Melaka, 75450 Ayer Keroh, Melaka, Malaysia*

ABSTRACT

Epoxidised natural rubber (ENR)-alumina nanoparticle composites (ENRAN) were produced by melt compounding followed by sulphur curing. Alumina nanoparticles were introduced in 10, 20, 30, 40, 50 and 60 parts per hundred rubbers (phr) in the formulations to study the effect of filler loading on the tensile properties. The fracture surfaces of ENRANs were studied using scanning electron microscopy (SEM). The increase in alumina nanoparticles content in the ENR matrices resulted in the decrease of the tensile strength and the elongation at break (EB) but increased the tensile modulus compared to unfilled ENRs. The reinforcement of alumina nanoparticles in ENR matrices is evident by the increase of crosslink density and glass transition temperature, Tg with increasing alumina nanoparticles content. The SEM micrographs showed the ENRANs were failed in primarily brittle mode when loaded with high filler loading. The alumina particles were observed to be uniformly distributed in the matrices which contributed to the enhancement of the tensile modulus. When present in the matrix, the particles formed spheres of agglomerates thereby enhancing filler-matrix interaction which also contributed to the reinforcement effect.

INTRODUCTION

Much research has been carried out in the development of nano-filled composites through the incorporation of nano-scaled materials such as ceramics and carbon in polymer matrices. For instance, organoclays [1], carbon nanotubes [2], alumina nanoparticles [3] and silica nanoparticles [4] have been previously added to polymers as fillers. Polymer nanocomposites exhibit unique properties even by the addition of low weight percent nanofillers (<5 wt%), that cannot be obtained from conventional or micro-scale fillers [5]. The incorporation of nanofillers enhances the mechanical, electrical, optical and other properties of polymer composites without sacrificing too much of the good properties such as the toughness being traded for the stiffness as found in rubber filled carbon fibres [6]. Several polymers have been used for preparing polymer nanocomposites such as elastomers (natural rubber, epoxidised natural rubber,

Corresponding Author: noraiham@vlsi.eng.ukm.my

styrene-butadiene rubber, chloroprene rubber, ethylene propylene diene monomer rubber etc.), thermoplastics (nylon 6, 6, polypropylene, polyethylene terephthalate, polymetylmetacrylate, polycarbonate etc.), and polymer blends.

The development of polymer-ceramic nanocomposites has created a number of technologies and opportunities that can be applied to epoxidised natural rubber (ENR). In a previous research by Teh et al.[1], ENR was used as a compatibiliser in producing natural rubber-organoclays nanocomposites. Organoclays can be more easily dispersed in polar polymers compared to non-polar polymers such as natural rubber (NR) [1]. ENR is miscible with more polar polymers [7] thereby offering unique properties such as good oil resistance, low gas permeability, higher wet grip, rolling resistance, and a high strength. The oil resistance of ENR 50 vulcanisate was reported to approach the characteristics of medium-acrylonitrile-content nitrile rubber and also surpassed that of chloroprene rubber (CR) [7]. The resistance to air permeability of ENR 50 has also been claimed to be comparable to butyl rubber and medium-acrylonitrile-content nitrile rubber [7]. Alumina has been recognised as a structural material with an extremely high melting point (2050°C), high hardness, and capable to take on diverse shapes and functions [8]. The incorporation of nano-scaled alumina in polypropylene (PP) has improved the mechanical properties of the polymer composites [9] and increased the wear resistance of polyethylene terephthalate (PET) filled alumina nanoparticles by nearly 2× over the unfilled polymer [10].

The ENR-alumina nanoparticles composites can be prepared using procedures as those used for NR. Rubber nanocomposites with an exfoliated morphology have been successfully prepared by several methods such as in situ polymerisation, solution blending, and direct melt compounding [11]. The solution method is widely used to prepare nanocomposites, which can be applied to ENR but this method is very inconvenient due to the use of organic solvents [12]. Hence, the melt compounding method using the internal mixer has been used to synthesise ENR-alumina nanoparticles composites.

METHODOLOGY

Materials

Table 1 shows the formulation used in this study. In these recipes, the content of alumina nanoparticles were varied as 10, 20, 30, 40, 50 and 60 phr whereas the rubber and other ingredients were kept constant. Epoxidised natural rubber was supplied by the Malaysian Rubber Board under the trade name ENR 50 with 53% epoxidization. The Mooney viscosities measured at ML (1 + 4) 100°C was 85.5. Alumina nanoparticles were obtained from Nanostructured & Amorphous Materials Inc., USA with size ranging from 30-80 nm. Sulphur, zinc oxide, and stearic acid were purchased from Systerm/Classic Chemicals Sdn Bhd, Tetramethylthiuram disulfide (TMTD) from Aldrich Chemistry and other chemicals such as N-cyclohexylbenthiazyl sulphenamide (CBS) and N-(1,3-Dimethylbutyl)-N'-phenyl-p-phenylenediamine (6PPD) were supplied by Flexsys America, USA.

Corresponding Author: noraiham@vlsi.eng.ukm.my

Solid State Science and Technology, Vol. 17, No 2 (2009) 133-143
ISSN 0128-7389

Table 1: ENRAN compounding recipe

INGREDIENTS	LOADINGS (phr)[a]
ENR 50	100
Sulphur	1.6
Zinc oxide	2.0
Stearic acid	1.5
CBS[b]	1.9
TMTD[c]	0.9
6PPD[d]	2.0
Alumina	10, 20, 30, 40, 50, 60

[a] Parts per hundred rubber
[b] N-cyclohexylbenthiazyl sulphenamide
[c] Tetramethylthiuram disulfide
[d] N-(1,3-Dimethylbutyl)-N'-phenyl-p-phenylenediamine

Mixing & cure characteristics

The compounding process was performed according to ASTM D-3192 and carried out using an internal mixer (Haake) working at 80°C and a rotor speed of 50rpm for 5 min. Firstly, ENR was masticated for 1 min before all ingredients except sulphur were added and mixed for another 3.5 min. Finally, sulphur was added and mixed for about 1 min before the mixture was dumped and cooled down to room temperature.

From this stock, unvulcanised samples were cured using a semi efficient vulcanisation (EV) system in a hot press at 150°C at the respective cure times, t_{90} which was derived from rheometer tests in a previous study [13].

Tensile properties

Tensile tests of the vulcanised samples were carried out according to BS 6746 using a Universal Testing Machine (Instron 4301) at room temperature and at a cross-head speed of 500mm/min.

Swell measurements

Cured test pieces of dimension 30 x 20 x 1 mm were swollen in toluene (solvent) for 24 hours at room temperature. Q (the weight of toluene absorbed per gram of rubber hydrocarbon) was determined according to Equation 1 [7]:

$$Q = \frac{Ws - Wds}{Wd\ X\ \frac{100}{Wt}} \quad (1)$$

where *Ws* is the swollen weight, *Wds* is the deswollen weight, *Wd* is the dry weight and *Wt* is the formula weight.

Corresponding Author: noraiham@vlsi.eng.ukm.my

Solid State Science and Technology, Vol. 17, No 2 (2009) 133-143
ISSN 0128-7389

Differential Scanning Calorimetry (DSC)
A differential scanning calorimetre (DSC) (Perkin Elmer Jade) was used to obtain the T_g of the vulcanised samples with a temperature ramp from -70 to 120 °C at 10 °C min^{-1}.

Scanning Electron Microscope (SEM)
The examination of the tensile fracture surfaces were carried out using a scanning electron microscope (ZEISS EVO 50) at magnifications of 500x and 5000x. For every sample, a minimum of three micrographs at each magnification were taken to ensure a high confidence level in the analysis. The distribution, shape and size of the dispersed alumina particles were also observed and analysed qualitatively. The micrographs were captured under variable pressure operated at 20 kV.

RESULTS AND DISCUSSION

Tensile properties
The tensile properties of the ENR filled and unfilled samples are shown in Figure 1 to 4. The tensile strength and the EB decreased as the alumina loading was increased. This result shows a different trend if compared to a previous research by Arroyo et al. [11]; since this present work involves a higher filler loading. In a research of low filler loading conducted by Ash et al. [14], the incorporation of 5 wt. % alumina nanoparticles into a polymethylmethacrylate (PMMA) matrix increased the average value of the strain-to-failure up to 600%. Normally, (in the case of conventional composites) the tensile strength will increase with increasing filler loading until a maximum point is reached; whereby the filler particles are no longer adequately separated or wetted by the rubber phase [15].

In the present work, the reduction in the tensile strength may have occurred due to the agglomeration of filler particles or simply the result of physical contact between adjacent agglomerates [15]. The agglomerate acted like a foreign body in the composites. Since there was a high amount of agglomerates in the higher filler loading composites, these agglomerates (refer to Figure 5) acted as obstacles to chains movement and could initiate failure under stress. This explained why the EB (Figure 2) showed the same trend as the tensile strength, which was to decrease with increasing amount of filler loading. The agglomerates became stress concentrators which build up stresses in the composites and eventually caused an earlier rupture compared to the unfilled samples. However, a different explanation was given by Ismail & Chia [7] who claimed that the poor tensile strength could have been attributed to the geometry of the fillers. The strength of the composites with irregularly shaped fillers decreased due to the inability of the fillers to support stresses transferred from the polymer matrices [16]. However, this could not have been possibly the cause for the decreasing tensile strength in the present study because the alumina nanoparticles formed sphere-like agglomerates (refer Figure 5 and 6) in the ENR matrices.

However, a loading of less than 10 phr of alumina nanoparticles in the ENR matrices

Corresponding Author: noraiham@vlsi.eng.ukm.my

might generate the same result as achieved by the other researchers [11, 16]; whereby the tensile strength increased with increasing filler loading. In the present work, the ability of the composites to withstand the tensile stresses during deformation decreased with decreasing ratio of rubber matrix to alumina fillers.

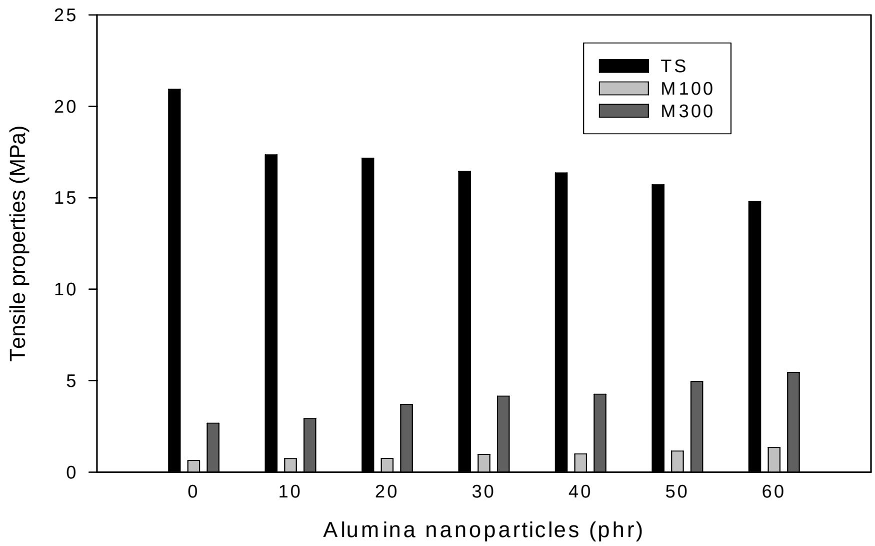

Figure 1: The effect of filler loading on the tensile strength, modulus at 100% elongation (M100) and modulus at 300% elongation (M300).

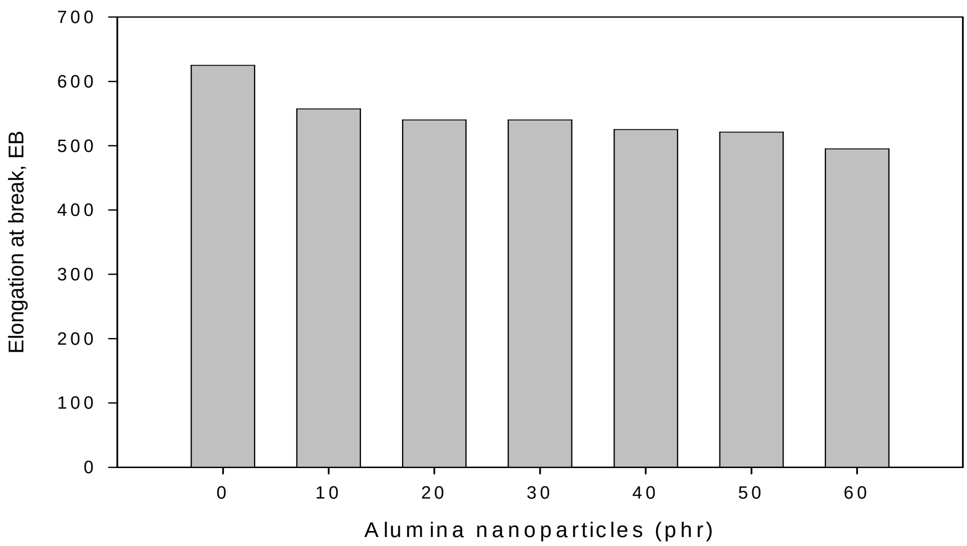

Figure 2: The effect of alumina nanoparticles loading on the elongation at break (EB)

In Figures 1 & 2, it is evident that the modulus at 100% and 300% elongation increases with increasing filler loading compared to the tensile strength and the EB of the composites. The increase of the tensile modulus may be attributed to the higher

Corresponding Author: noraiham@vlsi.eng.ukm.my

Solid State Science and Technology, Vol. 17, No 2 (2009) 133-143
ISSN 0128-7389

crosslink density and good distribution of fillers in the ENR matrices (Figure 5). It was proved by the weight of toluene uptake per gram of rubber,Q value determined by the swelling measurement. Figure 3 shows the relationship between Q against filler loading. It can be seen that the Q value decreases with increasing amount of alumina nanoparticles in the composites. Therefore, it can be reasonably assumed that the increase of the number of crosslinks which resemble three dimensional networks in the composites have lessened the capability of the composites to absorb toluene since there are fewer open chains in the composites for the toluene to penetrate. This suggested that alumina nanoparticles have helped for better crosslinking and at the same time contributed to an increase in the tensile modulus.

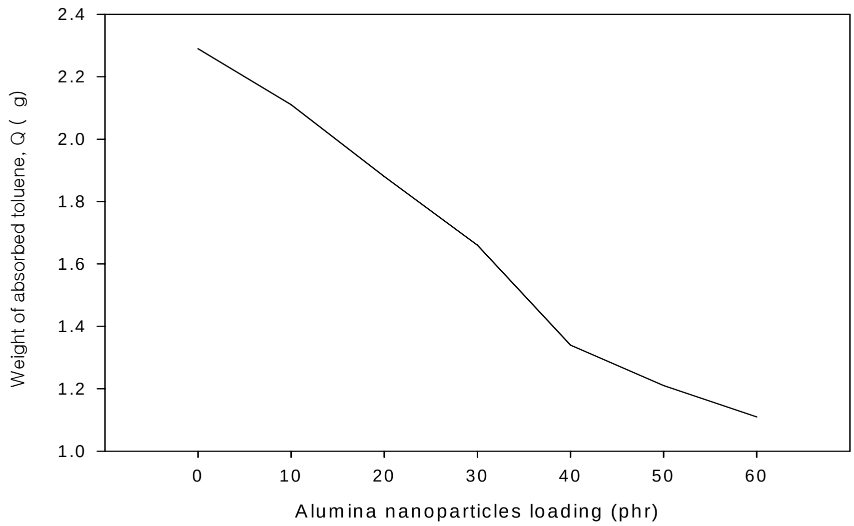

Figure 3: The weight of absorbed toluene per gram of rubber, Q for different phr of alumina loading.

The presence of polar groups in ENRs (epoxide groups) might have contributed to electrostatic adsorption between the ENR particles and alumina nanoparticles. This phenomenon was driven by different charges acting on the matrix or filler surfaces; which depends on the filler's type, pH value or inter-medium [17]. This mechanism would strengthen the polymer-ceramic interface. It would hold them together and increased their resistance to deformation. This helped in improving the modulus of the composites. The uniformity of the filler distribution also efficiently hindered the chain movements during deformation. This would increase the stiffness of the composites as well as the tensile modulus [18].

The reinforcement effects of the alumina nanoparticles on the ENRs also increased with increasing filler loading. This has been proven by the increase in glass transition temperature, Tg from -16.02°C for unfilled ENRs by almost 15% in ENR loaded with 60 phr alumina nanoparticles. The abrupt change was seen when the filler loading was increased from 10 to 20 phr followed by gradual increase up to filler loading of 60 phr. This is in good agreement with the morphology observed in Figure 5. The Tg almost

Corresponding Author: noraiham@vlsi.eng.ukm.my

Solid State Science and Technology, Vol. 17, No 2 (2009) 133-143
ISSN 0128-7389

reached its saturated value when the fillers were loaded with more than 20 phr in the ENR matrices; since it also depends on wettability of the components.

The increase in Tg is an indicator of the good adhesion between fillers and matrix [6]. According to Ajayan et al. [6] if a polymer is absorbed on the fillers surface, the glass transition temperature is stabilised or increase as large as 30°C. However, there are composites which experienced a decrease in the Tg as reported by Ash et al. [14] in their study on glass transition behaviour in alumina/PMMA nanocomposites. For the non-wetting nanoparticle/polymer composite (alumina/PMMA), the glass transition temperature starts to decerase at a specific filler volume fraction which can be as low as 0.5 wt.%. The alumina nanoparticles in their work acted as toughening agents rather than reinforcing materials for brittle PMMA since it increased the tensile ductility but decreased the tensile modulus.

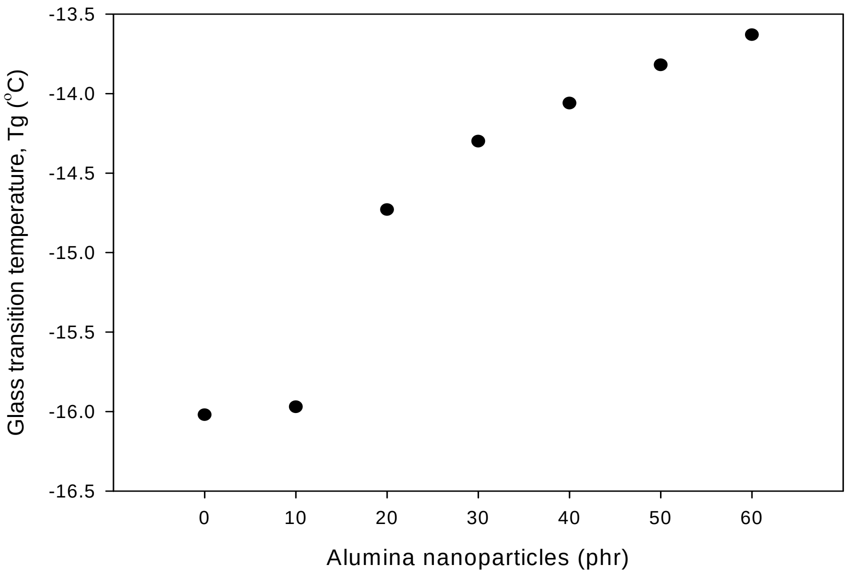

Figure 4: Tg versus alumina nanoparticles loading in ENRAN.

The changes in Tg of the composites can be caused by many factors; the interaction of the polymer chains with the surface of the particles which determine the interfacial region, changes in tacticity molecular weight, and retained monomer and interparticles distance [14]. The interfacial region is the region of polymer surrounding the nanoparticles and having altered chain conformation and/or mobility due to the presence of filler [6]. In these cases, the increase of Tg may be attributed to the large interfacial region generated between ENR and alumina nanoparticles which represent a good interaction. Larger interfacial region, narrower interparticles distance and higher crosslink density with increasing filler loading have restricted the cooperative motion among a large number of chain segments during deformation. As the results, the temperature where brittle to ductile transition increases with the addition of alumina

Corresponding Author: noraiham@vlsi.eng.ukm.my

Solid State Science and Technology, Vol. 17, No 2 (2009) 133-143
ISSN 0128-7389

nanoparticles in the composites.

Morphology of fracture surfaces and filler dispersion

Figure 5 and Figure 6 display SEM micrographs taken from the tensile fracture surfaces for unfilled and filled ENR at magnifications of 500x and 5000x, respectively. The dark phase represents the ENR matrix and the bright phase corresponds to the alumina particles. With the addition of nanoparticles and high strain rate at temperatures well above the Tg, the ENRAN fails in a primarily brittle fashion except for the unfilled ENR and those with lower filler loading. Considering the tensile mechanical data in Figure 1 and Figure 2 and having a look at the fracture surfaces in Figure 5. Most of the fracture surfaces show spherical shaped dimples from pull out of the alumina fillers except for the fractograph of unfilled ENR (refer to Figure 5 (a) and Figure 6 (a)). The fractograph of the unfilled ENR shows characteristics of ductile fracture under uniaxial tensile loads. When less than 20 phr alumina is added to the ENR matrix the surface roughness increases with increasing alumina loading. There is no obvious phase separation observed, implying good miscibility between ENR and alumina at this point. This is an indicator of good alumina–ENR adhesion. Fractograph in Figure 6 (b) for 10 phr filler loading shows similar contrast

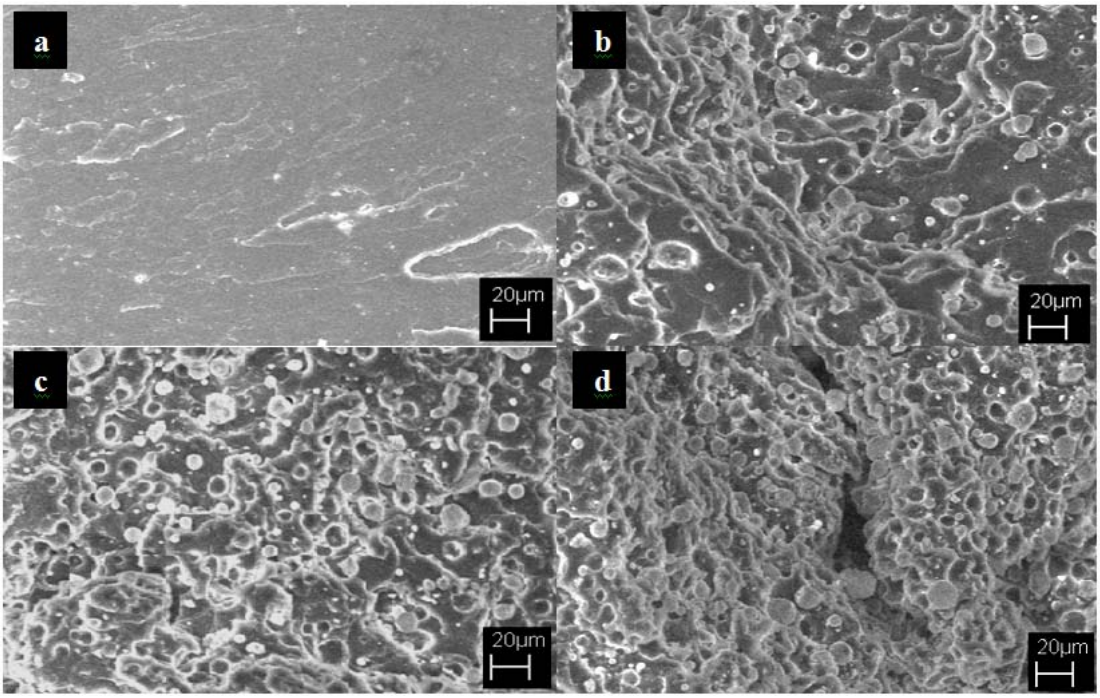

Figure 5: SEM fractographs using secondary electron at 500x magnification for (a) 0 phr (b) 20phr (c) 30 phr (d) 60 phr of alumina nanoparticles loading in the ENR.

Corresponding Author: noraiham@vlsi.eng.ukm.my

Solid State Science and Technology, Vol. 17, No 2 (2009) 133-143
ISSN 0128-7389

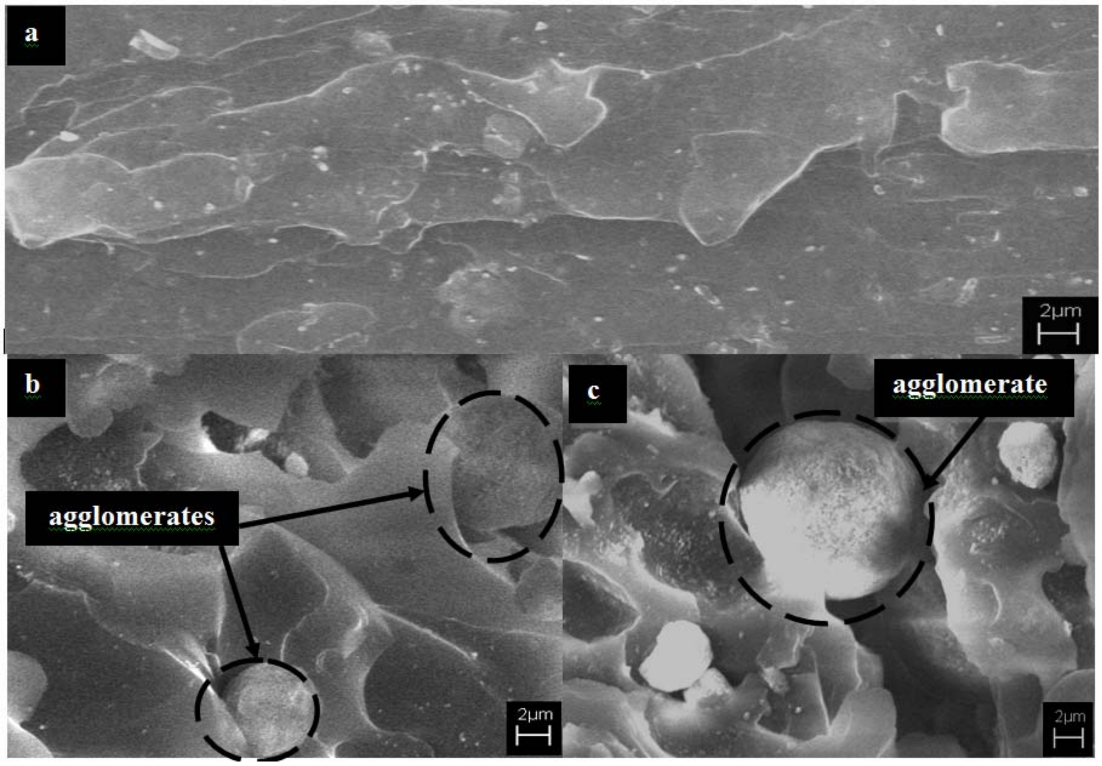

Figure 6: SEM fractographs under 5000x magnification for (a) unfilled ENR; ductile fracture. (b) 10 phr alumina loading. (c) 60 phr alumina loading; shows alumina agglomerates which act as foreign body and initiate crack during tensile deformation.

which represents a good adhesion between filler and matrix. It proves that the dispersed alumina nanoparticles in low filler loadings were fully encapsulated in the matrix even in the event of tensile pull out. However, the increasing surface roughness was not in line with decreasing tensile strength obtained. This may be due to agglomerations effect that occurred during compounding. Agglomerates acted as foreign body and initiated cracks in the composites under stress (refer to Figure 6(c)). The agglomerates reduced the tensile strength and the EB of the ENRANs. From the fractographs in Figure 5, surface roughness decreases with further increasing filler loading from 30 phr to 60 phr. The amount of agglomerates increases as the alumina content was further loaded. This may be due to the worsening wettability of the matrix onto the filler surface when the ratio of the fillers to the ENR matrix is too high, hence premature or brittle type fracture [1]. It can be observed in Figure 6(c) where the unwetted alumina agglomerate was solely present in between crack surfaces of high filler loading composite (60 phr). Composites with low filler loading showed higher tensile strength if compared to composites with higher filler loading since there were fewer agglomerates and better wettability in the composites.

Fractograph in Figure 5 shows alumina nanoparticles have uniformly distributed in the composites but poorly dispersed. There are fillers that form clusters (agglomerates) with

Corresponding Author: noraiham@vlsi.eng.ukm.my

size larger than original size of the starting alumina nanoparticles (30-80nm) presence in the composites. Although the size of agglomerates were big but sphere-like form has lessen their effect as stress concentrator in ENRANs. So, it did not show pronounced effect on tensile properties since it enhanced the tensile modulus.

CONCLUSIONS

The tensile strength and EB decrease with increasing alumina content in composites but increase the tensile modulus. Morphology of fracture surfaces shows that tensile properties are not only affected by crosslink density but also distribution, agglomeration and wettability. The presence of uniformly distributed alumina nanoparticles have effeciently hinder the polymer chain movements during deformation and contribute to the high stiffness of the composites.

ACKNOWLEDGEMENTS

The authors acknowledge the Ministry of Higher Education Malaysia and Universiti Kebangsaan Malaysia (UKM) for funding this research through the Fundamental Research Grant Scheme (UKM-RS-02-FRGS0003-2007). We wish to sincerely thank the Malaysia Nuclear Agency which provided the expertise, equipment and technical assistance while we conducted our experiments.

REFERENCES

[1] P.L. Teh, Z.A. Mohd Ishak, A.S. Hashim, J. Karger-Kocsis and U.S. Ishiaku (2004). Effects of epoxidized natural rubber as a compatibilizer in melt compounded natural rubber–organoclay nanocomposites. *Euro. Poly. J.* **40**, 2513–2521.

[2] A.M. Shanmugharaj, J.H. Bae, K.Y. Lee, W.H. Noh, S.H. Lee and S.H. Ryu (2007). Physical and chemical characteristics of multiwalled carbon nanotubes functionalized with aminosilane and its influence on the properties of natural rubber composites. *Compo. Sci. & Tech.* **67**, 1813–1822.

[3] R.W. Siegel, S.K. Chang, B.J. Ash, J. Stone, P.M. Ajayan, R.W. Doremus, and L.S. Schadler (2001). Mechanical behavior of polymer and ceramic matrix nanocomposites. *Scripta mater.* **44**, 2061–2064.

[4] S.J. Park, S.Y. Jin, and S. Kaang (2005). Influence of thermal treatment of nano-scaled silica on interfacial adhesion properties of the silica/rubber compounding. *Mater. Sci. & Eng. A.* **398,** 137–141.

[5] M.A. López-Manchado, J.L. Valentín, J. Carretero, F. Barroso and M. Arroyo (2007). Rubber network in elastomer nanocomposites. *Euro. Poly. J* **43 (10)**, 4143-4150.

[6] P.M. Ajayan, L.S. Schadler and P.V. Braun (2003). *Nanocomposite Science and Technology*. Weinheim: WILEY-VCH Verlag GmbH & Co. KGaA.

Corresponding Author: noraiham@vlsi.eng.ukm.my

[7] H. Ismail and H.H. Chia (1998). The effects of multifunctional additive and vulcanization systems on silica filled Epoxidized Natural Rubber compounds. *Euro. Poly. J*. **34(12)**, 1857-1863.

[8] I. Noboru (1987). *Introduction to Fine Ceramics (Application in Engineering)*. John Wiley & Sons Ltd.

[9] C.H. Jung, J.H. Choi, Y.M. Lim, J.P. Jeun, P.H. Kang and Y.C. Nho (2006). Preparation and Characterization of Polypropylene Nanocomposites Containing Polystyrene-grafted Alumina Nanoparticles. *J. Ind. Eng. Chem.* **12(6)**, 900-904.

[10] P. Bhimaraj, D.L. Burris, J. Action, W.G. Sawyer, C.G. Toney, R.W. Siegel and L.S. Schadler (2005). Effect of matrix morphology on the wear and friction behavior of alumina nanoparticle/ poly(ethylene) terephthalate composites. *Wear* **258**, 1437–1443.

[11] M. Arroyo, M.A. Lo´pez-Manchado, J.L. Valentı´n and J. Carretero (2006). Morphology/behaviour relationship of nanocomposites based on natural rubber/epoxidized natural rubber blends. *Compo. Sci. & Tech.* **67 (7-8)**, 1330-1339.

[12] Y.T. Vu, J.E. Mark, L.H. Pham and M.J. Engelhardt (2001). Clay nanolayer reinforcement of cis-1,4-polyisoprene and epoxidized natural rubber. *App. Poly. Sci.* **82(6)**, 1391-1403.

[13] N. Mohamad, A. Muchtar, M.J. Ghazali, H.M. Dahlan and C.H. Azhari (2008). Engineering Postgraduate Conference. Proc.

[14] B. J. Ash, L. S. Schadler and R. W. Siegel (2002). Glass transition behaviour of alumina polymethylmethacrylate nanocomposites. *Mat. Letters* **55**, 83-87.

[15] Z. A. M. Ishak and A. A. Bakar (1995). An Investigation on the potential of rice husk ash as fillers for Epoxidized Natural Rubber (ENR). *Euro. Poly. J.* **31(3)**, 259-269.

[16] H. Ismail and H.H. Chia (1998). The effects of multifunctional additive and epoxidation in silica filled natural rubber compounds. *Poly. Test.* **17**, 199–210.

[17] Z. Peng, L.X. Kong, S.D. Li, Y. Chen and M.F. Huang (2007). Self-assembled natural rubber/silica nanocomposites: Its preparation and characterization. *Comp. Sci and Tech.* **67**, 3130–3139.

[18] H. Ismail, H. D. Rozman, R. M. Jaffri and Z. A. Mohd Ishak (1997). Oil Palm Wood Flour Reinforced Epoxidized Natural Rubber Composites: The effect of filler content and and size. Euro. Poly. J.. **33, 10-12**, 1627-1632.

Corresponding Author: noraiham@vlsi.eng.ukm.my